THE MEAN FISSION-FRAGMENT RANGE IN BISMUTH AS APPLIED TO PULSE-TYPE ION CHAMBERS

LT. JAMES W. BEASLEY

THE MEAN FISSION-FRAGMENT RANGE IN BISMUTH AS APPLIED TO PULSE-TYPE ION CHAMBERS

by

James W. Beasley

This work is accepted as fulfilling

the thesis requirements for the degree of

MASTER OF SCIENCE

IN

PHYSICS

from the

United States Naval Postgraduate School

THE MEAN FISSION-FRAGMENT RANGE IN BISMUTH AS APPLIED TO PULSE-TYPE ION CHAMBERS

James W. Beasley

Lawrence Radiation Laboratory
University of California
Berkeley, California

May 15, 1959

ABSTRACT

The mean effective fission-fragment range in bismuth has been measured in order that thickness efficiency corrections may be computed for bismuth-fission ion chambers. Parameters affecting pulse-height distributions--such as Bi thickness, collecting voltage, and gas-filling pressure--were varied in order that the best discrimination between fission pulses and spallation pulses could be attained. Six parallel-plate pulse-type ion fission chambers were used with bismuth thicknesses ranging from no bismuth to 5.83 mg/cm^2. The relative efficiencies of these chambers were compared by using 212-Mev neutrons from the 184-inch Berkeley cyclotron, and it was determined that the mean effective fission-fragment range was 4.30 ± 0.40 mg/cm^2 in bismuth.

THE MEAN FISSION-FRAGMENT RANGE IN BISMUTH AS APPLIED TO PULSE-TYPE ION CHAMBERS

James W. Beasley

Lawrence Radiation Laboratory
University of California
Berkeley, California

May 15, 1959

INTRODUCTION

The bismuth fission chamber was conceived as a high-energy neutron detector (50 Mev or greater) by Clyde Wiegand.[1] It has subsequently been used in radiation and cosmic-ray surveys here at Berkeley.

This investigation was initiated in order that the results of these latter surveys might be more fully understood. During the course of the designing and running of this experiment, an attempt was made to vary conditions in such a manner that information might be obtained that will be of value in the design of future bismuth fission chambers.

Clyde Wiegand, in the testing of the first Bi fission chamber, came to the conclusion that only the outermost layer of Bi, 0.3 mg/cm^2, was effective in projecting fission fragments into the sensitive region of the chamber.[1] If this were the case, then the usefulness of this chamber would be greatly impaired because of the low efficiencies resulting from the limitation on the amount of effective bismuth one could place in a chamber without greatly increasing the chamber capacitance. Wilmot N. Hess et al. reported on a delay-line chamber with large plate areas, but a low output capacitance.[2] With this chamber, they were able to utilize 63 grams of Bi by coating both sides of all plates to a thickness of 1.0 mg/cm^2. With this chamber some difficulty was experienced in extrapolating the integral bias curves to zero bias.

Sugarman et al. measured the ranges in bismuth of Sr^{91}, Ba^{129}, and Ba^{133m} recoil fragments from the bombardment of bismuth with protons of 50 Mev to 2.2 Bev.[3] They reported ranges varying from 9.1 to 10.8 mg/cm^2 of Bi for Sr^{91} and 3.0 to 6.8 mg/cm^2 of Bi for $Ba^{129, 133m}$. These ranges were measured by means of radiochemical analysis of aluminum absorbers, and they represent the actual ranges of the fragments.

These reported ranges led me to suspect that the mean effective range, that range which would leave the fragment with sufficient energy to give a detectable amount of ionization in the chamber, would be somewhere between 0.3 mg/cm^2 and 9.0 mg/cm^2 of bismuth.

Particular attention has been given in this experiment to the differential pulse-height spectrum in order that spallation-produced pulses might be separated from true fission pulses. This allows the integral bias curve to be extrapolated to zero bias with minimum error.

FISSION-FRAGMENT-INDUCED IONIZATION

In contrast to the density of ionization produced by α particles, the density of ionization produced by fission fragments decreases with the distance traveled. This decrease occurs because the fragment, initially stripped of its electrons to a large extent, gains electrons rapidly as the fragment slows to a velocity on the order of the orbital electron velocity of the fragment.[4] The effective Z decreases, and ionization for heavy particles depends on Z^2.[5] N. O. Lassen observed also that the heavy group of fission fragments ionizes more than the light group at the beginning of the path, while in later parts of the path the heavy fragments ionized less than the light ones.[6]

Nyle G. Utterback et al. measured the ionization defect for fission fragments in an argon-plus-CO_2 mixture.[7] The ionization defects measured for the most probable light and heavy fragments of fissioned natural uranium were respectively 7.1 ± 1.0 Mev and 9.7 ± 1.2 Mev. Their explanation for this defect was based on the relative importance of elastic atomic collisions versus inelastic electron collisions. For very high particle velocities, inelastic electron collisions dominate as the mode of energy loss, but as the particle slows down, elastic collisions with other atoms becomes the dominant energy-loss process. For a particle of high nuclear charge, the velocity at which the elastic atomic collision becomes important is much higher than for particles of low nuclear charge. Therefore, elastic atomic collision is an important mode of energy loss for fission fragments over a large part of their range. In addition, if the recoil atoms from the elastic collisions are heavy, such as argon atoms, they absorb a large fraction of the energy of the fragment and still have a low recoil velocity. Because of this low velocity, the recoil atom is not efficient in producing secondary ionization. These effects were observed by K. J. Brostrøm et al. in a cloud chamber.[8] They observed branching due to nuclear collision occurring many times in a single track. Instead of pursuing a straight course to the ends of their ranges, the fragments exhibited large irregular curvature due to numerous collisions in which the momentum transfer in any single interaction was insufficient to give an observable branch.

Because of the dominant role that elastic collisions play in the energy loss process for low fragment velocities, the fragment would probably have to be projected into the sensitive region of the fission ion chamber with an energy somewhat greater than 10 Mev in order that it be counted as a fission event.

COUNTER EFFICIENCY

Consider a thin layer of bismuth of thickness t (see Fig. 1). The equation for the counter efficiency, neglecting momentum transferred to the bismuth nucleus, is clearly

$$dN(E, X) = \phi\, \sigma\,(E)\, nA \left[\int_0^{\cos^{-1} \frac{X}{R-r}} \sin\,\theta\, d\theta \right] dx dE, \qquad (1)$$

where ϕ = neutron flux,

$\sigma(E)$= fission cross section as a function of energy,

n = number of Bi atoms per unit volume,

A = area of Bi-coated plates,

(R-r) = range of fission fragment in bismuth minus the residual range required for a detectable event.

If Eq. (1) is integrated over θ, the result is

$$dN(E, X) = \phi\, \sigma\,(E)\, nA \left[1 - \frac{X}{(R-r)} \right] dx dE\,. \qquad (2)$$

Integrating Eq. (2) on X between the limits $0 \leq X \leq t$ gives

$$dN(E) = \phi\, nAt \left[1 - \frac{t}{2(R-r)} \right] \sigma(E) dE\,. \qquad (3)$$

Equation (3) is valid only for $t \leq (R-r)$. If it is assumed that σ is independent of energy or that a monoenergetic neutron flux is used, the counting rate is

$$N = \phi \sigma\, nAt \left[1 - \frac{t}{2(R-r)} \right]\,. \qquad (4)$$

The quantity in brackets is the thickness correction for efficiency, and if this function is plotted versus t, the value (R-r) can be determined by the value of t at which the thickness correction is equal to 0.5.

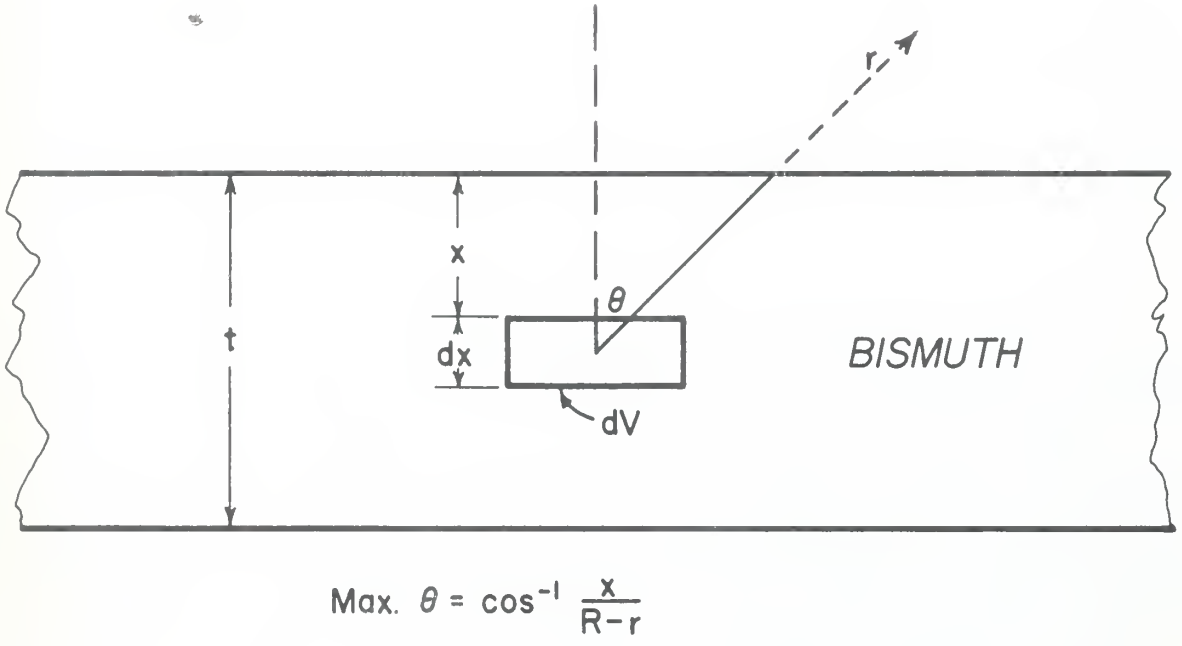

Fig. 1. Representation of parameters used in computing counter efficiency with a thin layer of bismuth.

Equation (4) is the basic working equation for this experiment, and the basic quantity to be measured is the mean effective range of the fragment, defined from here on as (R-r).

DIFFERENTIAL PULSE-HEIGHT SPECTRUM

Calculated differential pulse-height spectra for various thicknesses of bismuth coatings are shown in Fig. 2. (The calculations are included in Appendix I.)

Several simplifying assumptions were necessary in deriving these curves. It was first assumed that all fission fragments have the same mass and energy as the most probable fission fragment. Goeckermann and Perlman, in fission-yield experiments on bismuth, have determined that the most probable mass number is 99 and that the yield curve probably is symmetrical about this mass number.[9] Next it was assumed that the range-energy relation

$$E = kR^2$$

was valid for the fission fragments in both bismuth and the gas. Sugarman et al. used this relation in their recoil experiment to determine the initial kinetic energies of the Sr^{91}, Ba^{129}, and Ba^{133m} recoil fragments.[3] Lassen has shown this relationship to be true only for heavy fragments (A = 139) in argon.[6] For lighter fragments (A = 95) the curve for dE/dR versus R has a small slope for small R, with the slope increasing as R increases. The final simplifying assumption was that all the fission-fragment kinetic energy went into ionization of the gas. It was pointed out in the section on Fission-Fragment-Induced Ionization that this is not entirely correct.

It can be seen from Fig. 2 that in order to discriminate between spallation pulses (pulse heights ranging up to about 25 volts) and fission pulses, the layer of bismuth must be kept thin relative to the mean effective range of the fission fragments. Also, the calculated peaks are much better defined than those which are observed experimentally, because of the simplifying assumptions made in the calculations, and experimentally some broadening of the peaks can be expected due to pileup of small spallation pulses on the fission pulses.

The curves for experimental differential pulse-height spectra are shown in Figs. 3 and 4. Figure 3 includes spallation-produced pulses and in Fig. 4 an attempt has been made to subtract the spallation-produced pulses. Because of unavoidable differences in chamber gain, the relative positions of the peaks on the pulse-height scale do not agree with those on the computed curves.

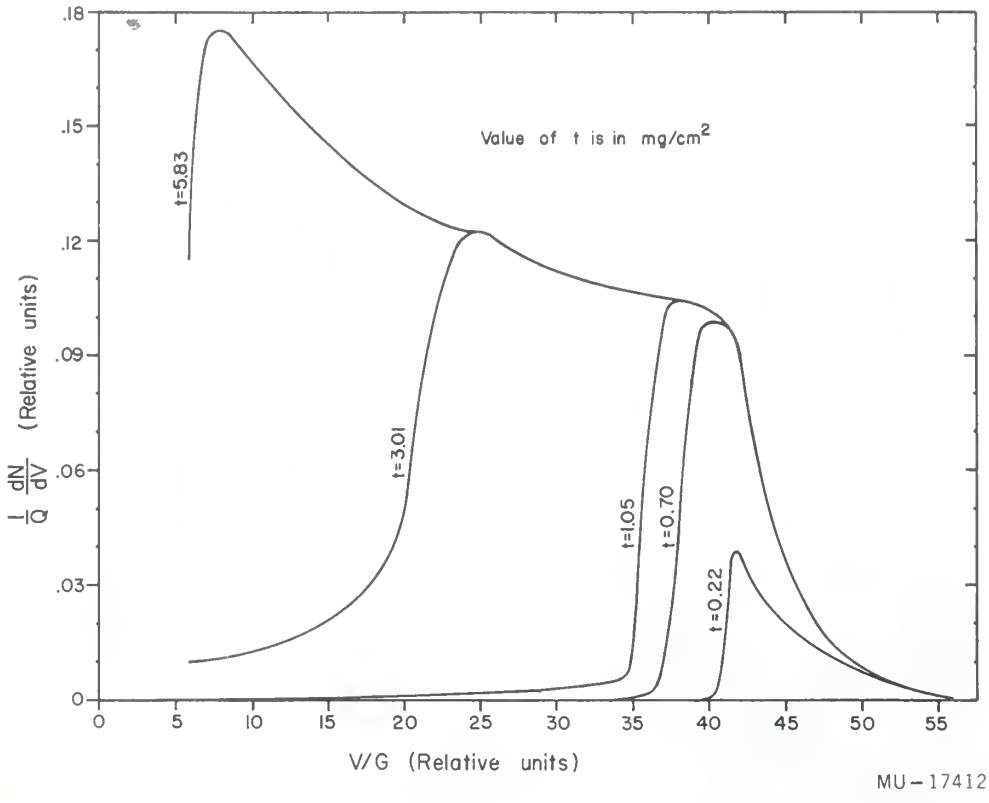

Fig. 2. Computed differential pulse-height spectra for different thicknesses of bismuth. $Q = \phi \sigma n A$, and $(R - r)$ assumed to be 9.2 mg/cm^2.

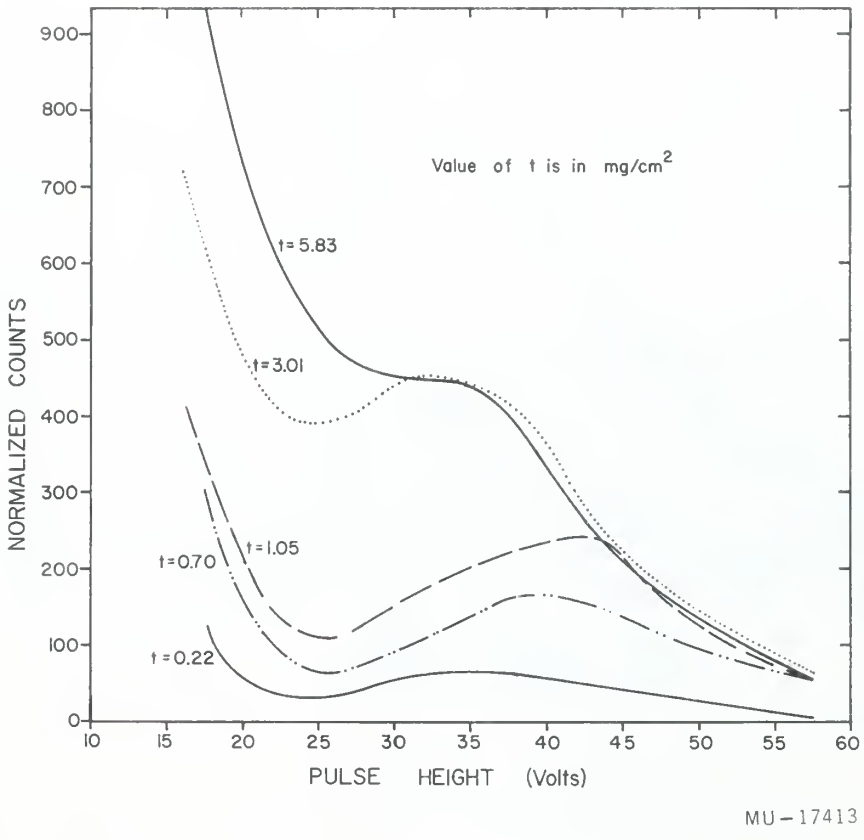

Fig. 3. Experimental differential pulse-height spectra (uncorrected).

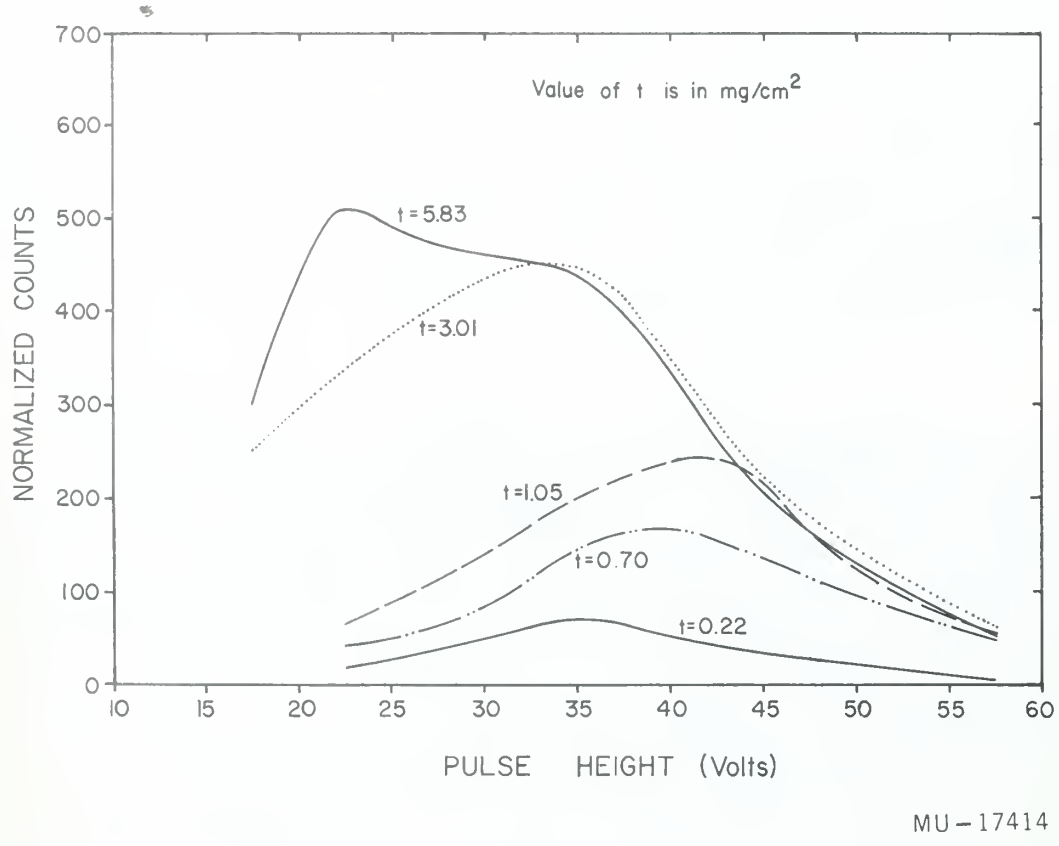

Fig. 4. Experimental differential pulse-height spectra with spallation-produced pulses subtracted.

APPARATUS

A. Fission Ion Chambers

a. Construction

A schematic drawing of one of the pulse ion chambers used is shown in Fig. 5. Each chamber has 30 aluminum plates, alternate plates having had bismuth evaporated to the same thickness onto both sides. Six chambers were used, each containing a different thickness of bismuth. The thicknesses used were; 0, 0.22, 0.70, 1.05, 3.01, and 5.83 mg/cm^2. The area of each plate was 18 cm^2, and the spacing was 1.19 cm. Trimming capacitors (not shown in Fig. 1) were used in the signal output to make the chamber capacitances all equal to 130 micromicrofarads.

b. Gas Filling

The chambers were filled to a pressure of 1 atmosphere with a mixture of 96% argon and 4% carbon dioxide. This provides approximately 2 mg of gas path length when the fragment path is perpendicular to the plates. The addition of CO_2 to argon decreases the electron-collection time by increasing the electron drift velocity. This is explained for argon on the basis of the Ramsauer effect and the first excitation level of argon, 11.5 volts, in comparison with the low excitation levels of the CO_2 molecule.[10] Electron collection was utilized in order that the fission pulses might have a rise time of about 0.5 microsecond. Gas pressures of 1/2 and 1-1/2 atmospheres were also used with a representative chamber in order that the effect on the pulse-height distribution might be observed.

c. Collecting Voltage

The high positive voltage was applied to the collecting electrode, and the chamber walls and bismuth-coated plates were maintained at ground potential. This configuration was used in order that the electric field in the chamber would be well defined. The high voltage used was 600 volts, which was well on the voltage-vs-counts plateau. See Fig. 6.

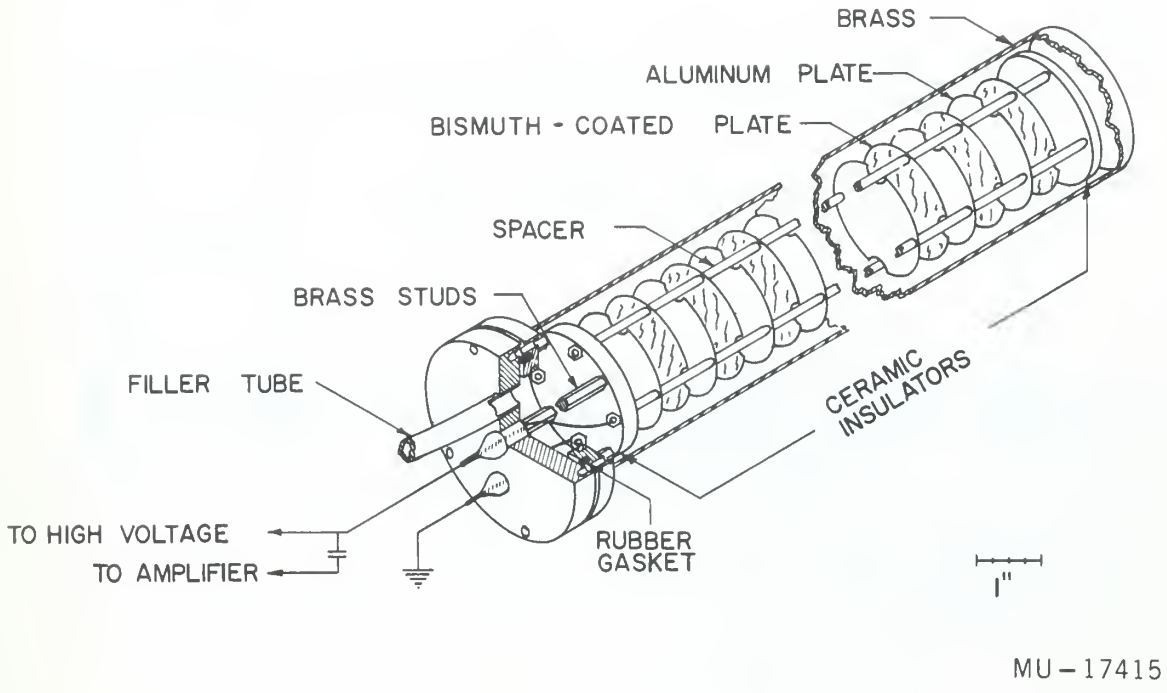

Fig. 5. Schematic drawing of the bismuth-fission pulse-type ion chamber.

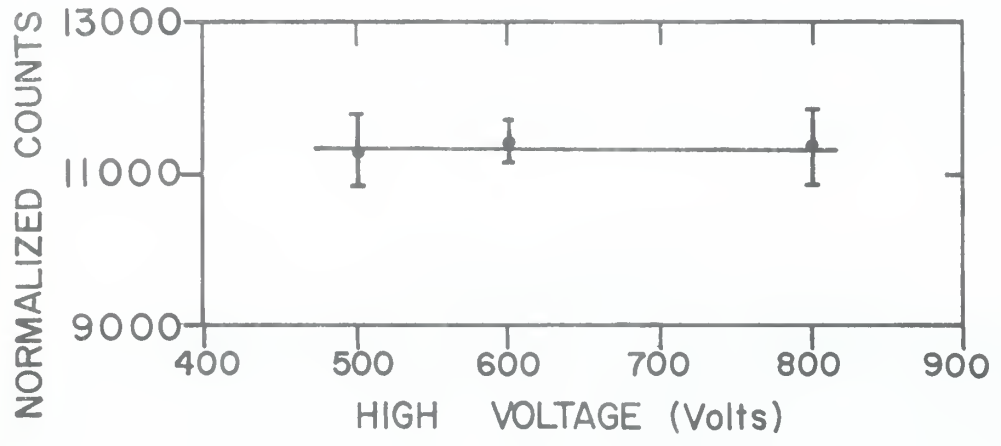

Fig. 6. Counter high-voltage plateau.

B. Electronics

A schematic diagram of the electronics is shown in Fig. 7. Because of the fast rise time of the fission pulses, severe differentiation could be applied in the amplifier circuits. The short decay time of pulses (about 6 microseconds) and the fast rise time of the pulses made the amplifier insensitive to microphonics and ordinary mechanical vibration.

The pulse-height analyzer used had 10 channels with an extra integral channel which was used to count all pulses above the highest channel. The low-level discriminator in the first channel was set at 10 volts and the window widths were set for 5 volts. This gave a differential spectrum from 10 to 60 volts and an integral count above 60 volts.

C. Beam Monitor

A previously calibrated bismuth fission chamber with an unknown thickness of bismuth (on the order of 1 mg/cm^2) was used to monitor the beam. This chamber was monitored by two scalers, each with a different discriminator setting. By application of a correction factor to either of these scalers the number of counts at zero bias can be obtained for the monitor chamber.

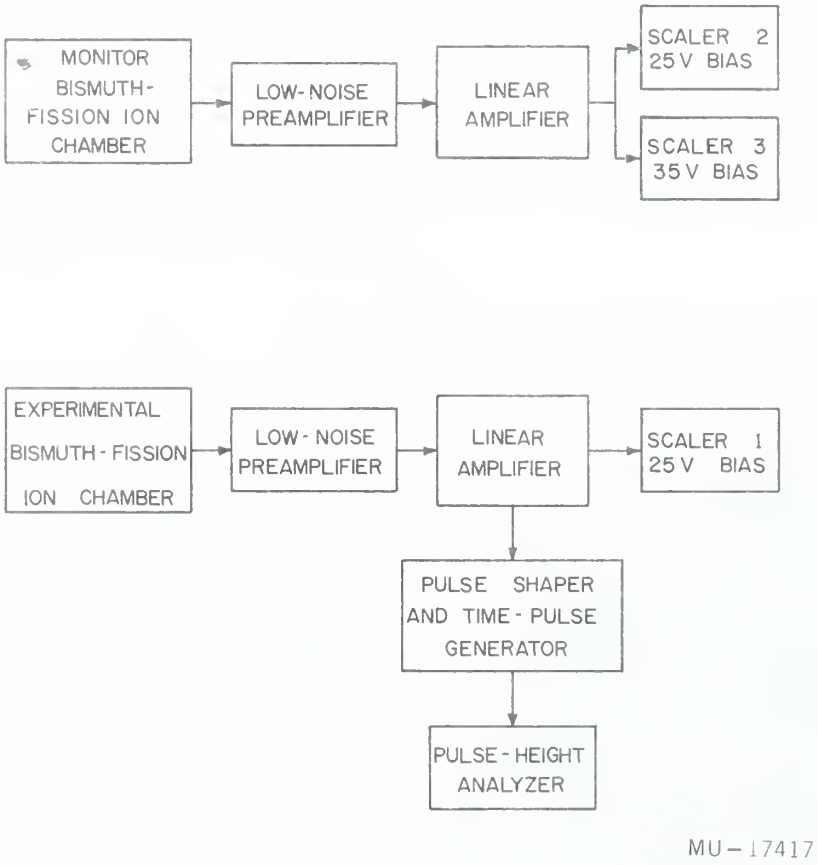

Fig. 7. Block diagram of the electronics

EXPERIMENTAL METHOD AND PROCEDURE

A. Arrangement

The general experimental arrangement at the 184-inch Lawrence Radiation Laboratory Synchrocyclotron is shown in Fig. 8. The neutron beam used was produced by the bombardment of a 2-inch beryllium target with accelerated deuterons. The deuteron energy was 455 Mev and, according to Serber,[11] this should give a narrow beam of neutrons with a mean energy of 212 Mev. In order to have a maximum solid angle for the beam where the fission chambers were mounted, all collimators were removed from the neutron port.

B. Procedure

1. Alignment

The alignment of the fission ion chambers with respect to the beam was accomplished by the use of photographic film. This alignment was checked and the structure of the beam determined by placing 30 small carbon disks throughout the profile of the beam in a known position with respect to the fission chambers. These disks were exposed to the neutron beam for 45 minutes, and then the $C^{12}(n, 2n)C^{11}$ activation of each disk was checked by counting the beta decay of C^{11} to B^{11}, with a methane gas-flow proportional counter. This check showed the beam intensity to be almost uniform across the beam profile determined with photographic film as shown in Fig. 9.

2. Spallation Pulses and Background

It was found that if the count rate was too high, considerable pileup of spallation pulses occurred. This effect could be observed by displaying the pulses at the output of the linear amplifier on an oscilloscope, and under this condition the differential pulse-height spectrum would fail to show a peak. This pileup effect was minimized by using a beam intensity which would give less than 150 fission counts a minute, when the beam-spill time was between 350 and 400 microseconds. If the spill time

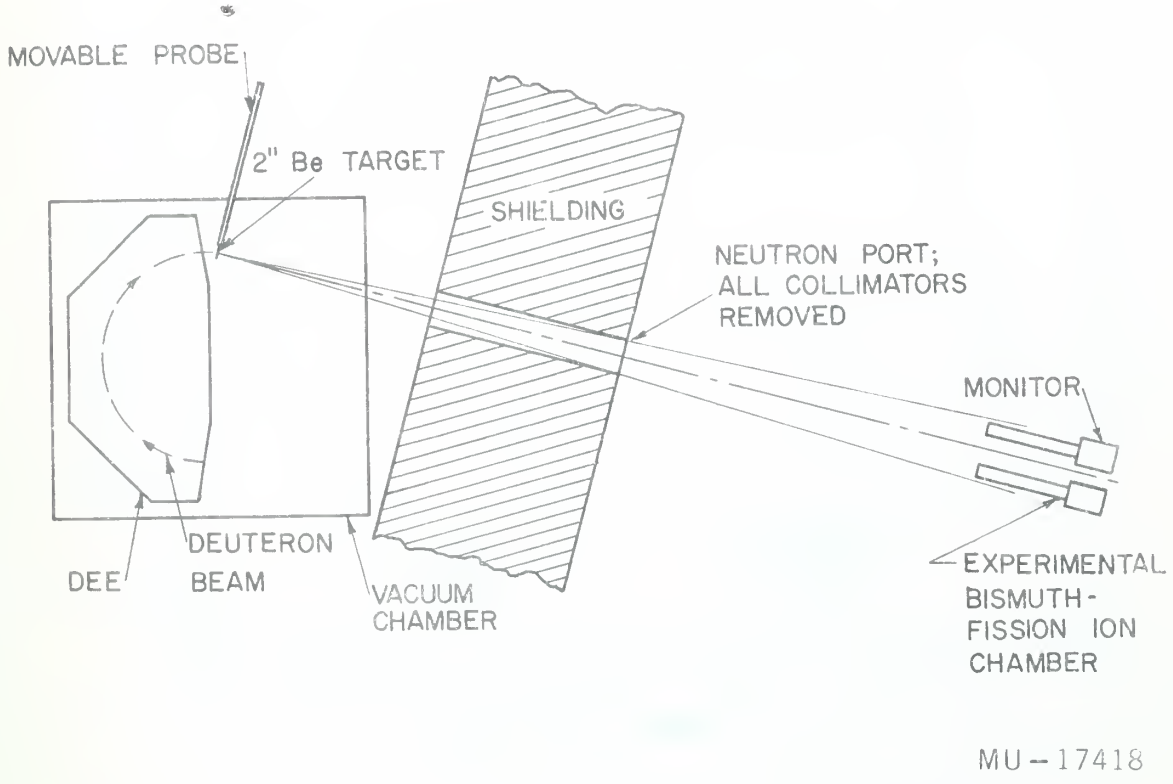

Fig. 8. Schematic diagram of the experimental arrangement at the cyclotron. (Not to scale.)

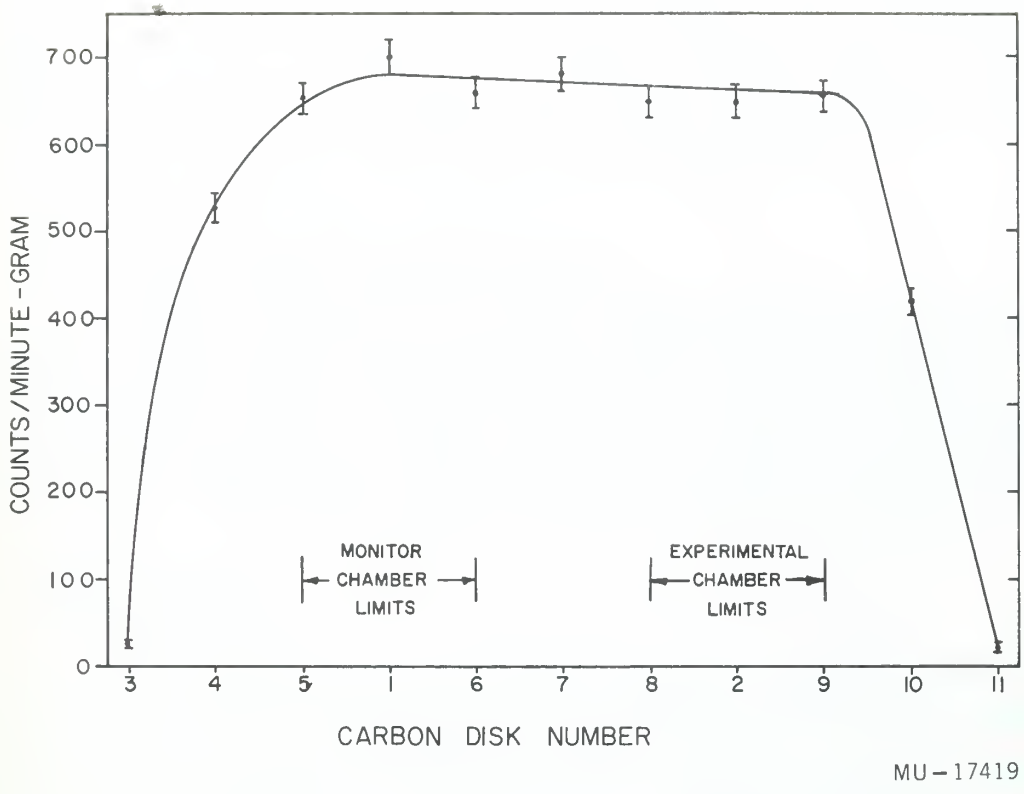

Fig. 9. Neutron beam structure determination using the $C^{12}(n, 2n)C^{11}$ reaction.

decreased, the maximum count rate had to be correspondingly decreased in order to prevent spallation-pulse pileup.

Background is considered to be negligible because with the beam off no counts were observed in either the monitor or experimental chamber when they were checked for a period of 1 hour.

Spallation pulses are due predominantly to the bismuth in the chamber. This was shown by using a chamber with no bismuth on the aluminum plates. No pulses were observed greater than 30 volts. Figure 10 shows a comparison between this dummy chamber and the 0.70-mg/cm^2 chamber run under identical conditions.

3. Variation of Gas-Filling Pressure

In order to determine the gas-filling pressure that would give the best discrimination between spallation pulses and fission pulses, the 1.05-mg/cm^2 chamber was operated at three different filling pressures. It is evident from Fig. 11 that 1 atmosphere gives the best-defined fission peak. This was the pressure used for this experiment.

4. Data Analysis

Integral bias curves were taken for each chamber on each experimental run. These curves were extrapolated to zero bias by subtracting out the spallation spectrum (see Fig. 12), and the number of counts so attained was normalized to 10,000 monitor counts at 25 volts bias. From the equation for the computed efficiency, we have

$$N = \phi \sigma n A t \left(1 - \frac{t}{2(R-r)}\right) \quad \text{for} \quad t \leq (R-r);$$

the quantities ϕ, σ, n, and A were the same for all chambers because of the similarity of the chambers, the running conditions, and the normalization used. N/t could then be computed for each thickness and a direct comparison made of the quantity $\left(1 - \frac{t}{2(R-r)}\right)$ for each thickness. Results from the chambers with $t \geq 0.22$ mg/cm^2 were compared with the 0.22-mg/cm^2 chamber. On the assumption that the 0.22-mg/cm^2

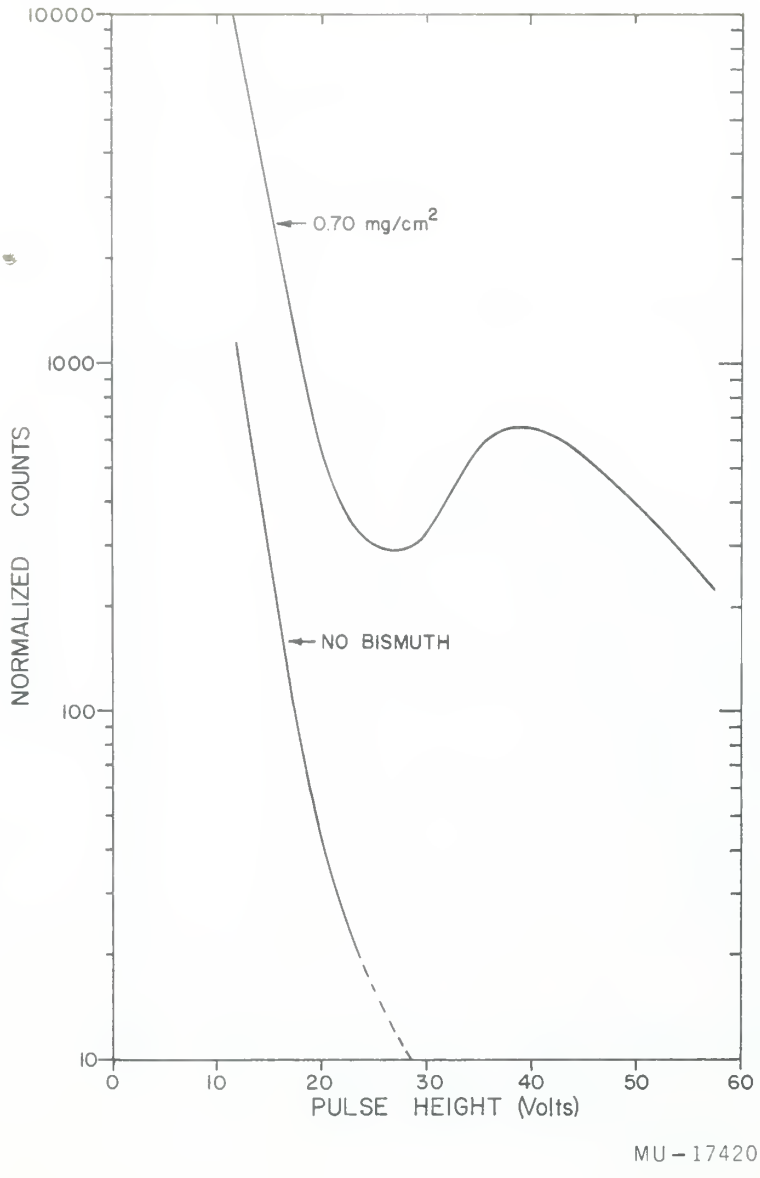

Fig. 10. Comparison of the differential pulse-height spectra for the no-bismuth and 0.70-mg/cm^2 chambers.

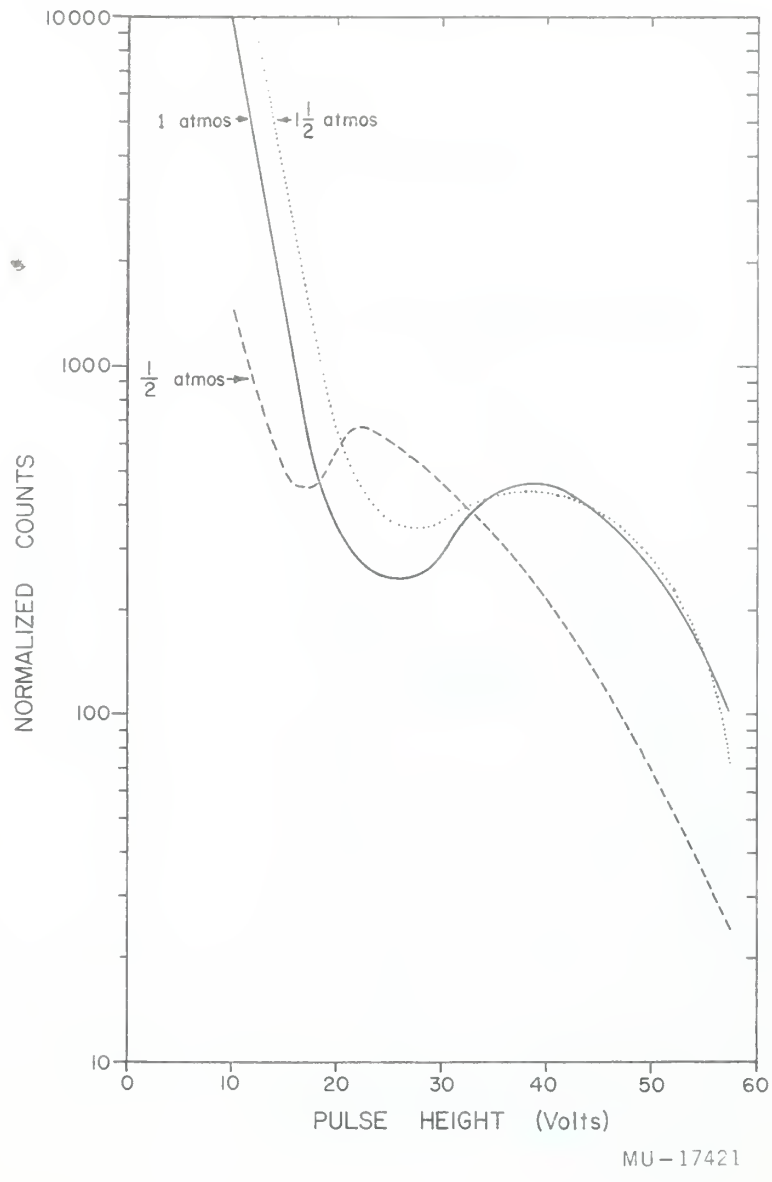

Fig. 11. Differential pulse-height spectra of the 1.05-mg/cm^2 chamber for gas-filling pressures of $\frac{1}{2}$, 1, and 1 $\frac{1}{2}$ atmospheres.

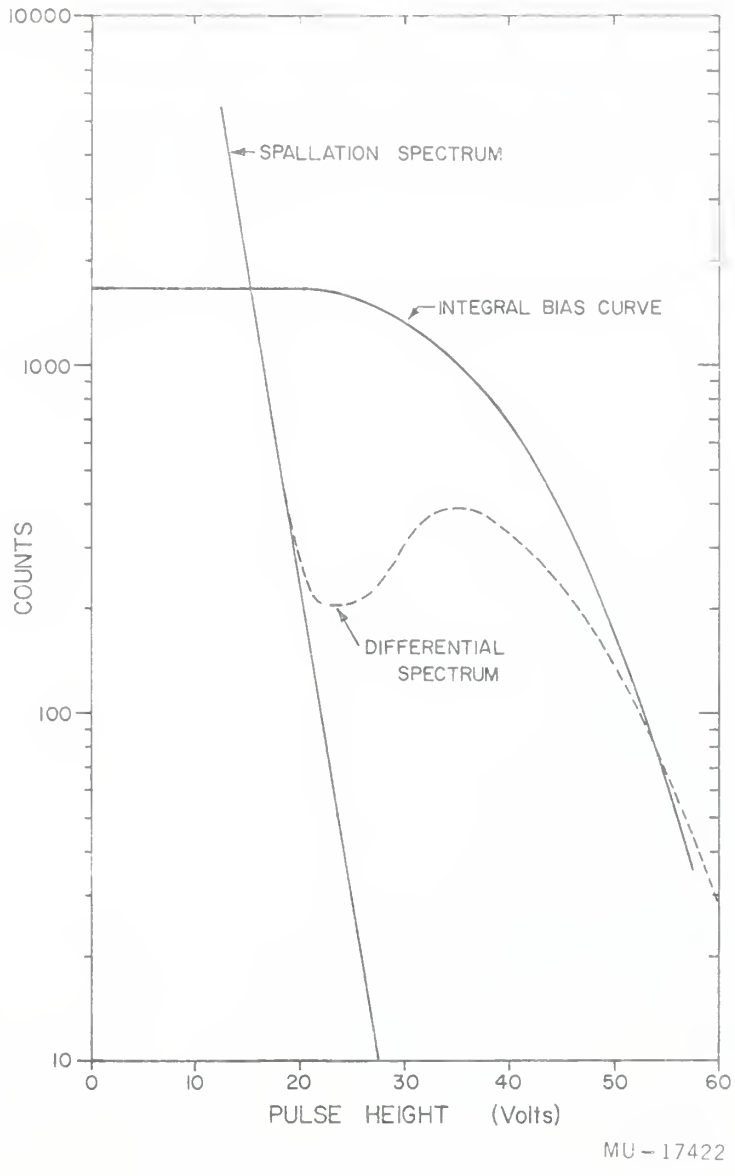

Fig. 12. Method used to extrapolate the integral bias curves to zero bias, i.e., the spallation spectrum was subtracted from the differential spectrum in calculating the integral bias curve.

chamber was 100% efficient, the quantity (R - r) was computed and this value was used to determine the thickness-correction factor for the 0.22-mg /cm^2 chamber. This allowed the chamber comparisons to be normalized to t = 0, and the final value of (R-r) could then be determined. See Fig. 13. It is to be noted that no point is plotted for t = 5.83 mg/cm^2. This is because the equation upon which this graph is based is valid only for $t \leq (R - r)$

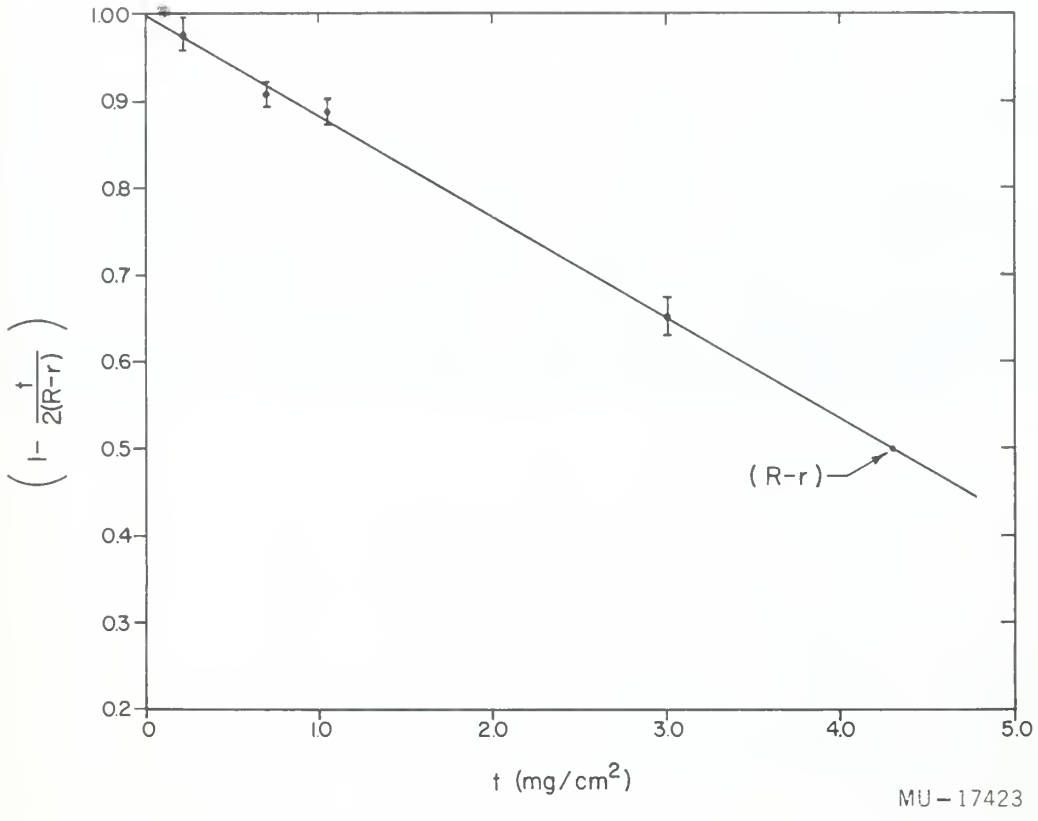

Fig. 13. Experimental plot of $\left[1 - t/2(R-r)\right]$ versus t.

RESULTS AND CONCLUSIONS

The mean effective fission-fragment range was found to be 4.30 ± 0.40 mg/cm^2 of bismuth. The plot of t versus $\left[1 - t/2(R-r)\right]$ from which this value was determined is shown in Fig. 13. The error given is due to counting statistics only.

The principal reason for measuring the mean effective fission-fragment range in bismuth is to provide information on how thick a layer of bismuth might be used efficiently in a bismuth fission chamber. It appears that a layer 2 mg/cm^2 thick can be used efficiently without losing discrimination between fission pulses and the spallation-produced pulses. This conclusion is based on the assumption that bismuth is coated only on alternate plates, and that electron collection occurs on a set of plain plates. This gives a maximum displacement for the negative ions (electrons) with resulting larger pulses.

ACKNOWLEDGMENTS

This work was conducted under the guidance of Dr. Roger W. Wallace and Dr. Wilmot N. Hess at the University of California Lawrence Radiation Laboratory as part of the Special Physics Curriculum of the U.S. Naval Postgraduate School, and done in part under the auspices of the U.S. Atomic Energy Commission.

In addition to the above named, I wish to thank Mr. Wade Patterson and Mr. Alan R. Smith for providing me with background information and helpful suggestions; Mr. Lloyd D. Stephens and Mr. Joseph B. McCaslin for their help during the experimental runs; and the staff of the 184-inch synchrocyclotron under the direction of Mr. James Vale for their helpfulness throughout the course of the experiment.

It is with pleasure that I acknowledge the wholehearted cooperation extended to me by Professor Burton J. Moyer and his entire group.

APPENDIX

CALCULATION OF THE DIFFERENTIAL PULSE-HEIGHT SPECTRUM

Let R_0 = total range of the most probable fission fragment in bismuth,
E = initial kinetic energy of the fission fragment,
E' = kinetic energy of the fission fragment as it enters the sensitive region of the chamber,
R' = range of the fission fragment in the sensitive region of the chamber,

and

$$E = k_1 R_0^2,$$
$$E' = k_2 F'^2.$$

Then we have

$$E' = E - \int_{R_0 - r}^{R_0} 2k_1 R \, dR,$$

$$E' = E + k_1 r^2 - 2k_1 r R_0,$$
$$E' = E + \frac{k_1 \chi^2}{\cos^2 \theta} - \frac{2k_1 R_0 \chi}{\cos \theta} . \qquad (1)$$

Letting V represent pulse height, E_ℓ the energy given up to the gas in a path length ℓ, and G a gain constant, we can write

$$dV = G \frac{dE_\ell}{d\ell} \left(\frac{D - \ell \cos \theta}{D} \right) d\ell , \qquad (2)$$

where

$$E_\ell = k_2 (R' - \ell)^2 ,$$

$$E_\ell = k_2 \left[\frac{E'}{k_2} - 2\ell \sqrt{\frac{E'}{k_2}} + \ell^2 \right];$$

then

$$\frac{dE_\ell}{d\ell} = - 2k_2 \sqrt{\frac{E'}{k_2}} + 2k_2 \ell . \qquad (3)$$

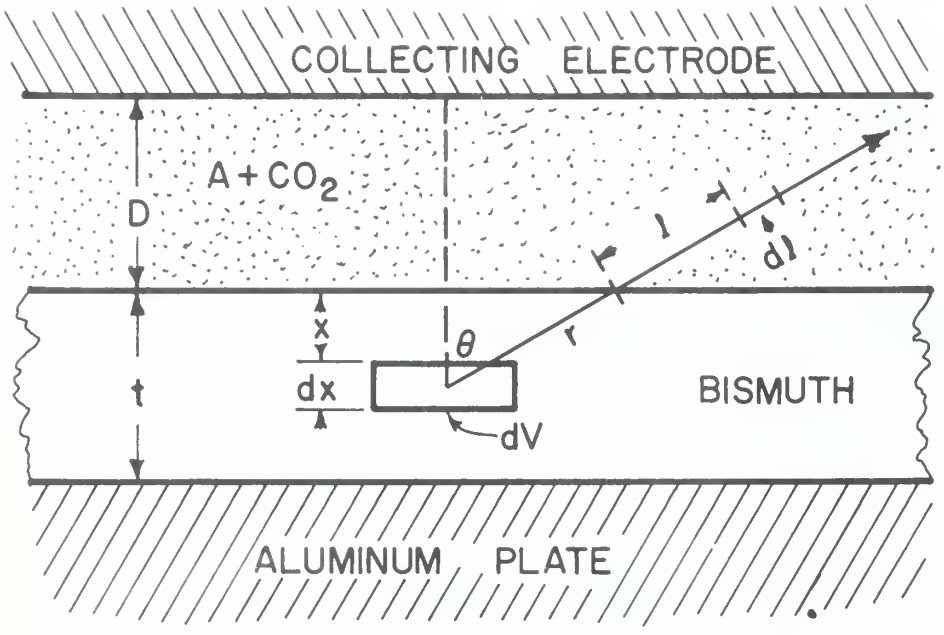

Fig. 14. Representation of parameters used in computing differential pulse-height spectrum.

Substituting Eq. (3) into (2) gives

$$dV_\ell = G\left[-2\sqrt{k_2 E'} + \frac{2\sqrt{k_2 E'}\cos\theta\,\ell}{D} + 2k_2\ell - \frac{2k_2\ell^2\cos\theta}{D}\right] d\ell \ . \quad (4)$$

If Eq. (4) is integrated on ℓ between the limits 0 and R', and E' is eliminated by using Eq. (1), we have an expression for the pulse height as a function of χ and θ:

$$V/G = \frac{\cos\theta}{3D\sqrt{k_2}}\left[E + \frac{k_1\chi^2}{\cos^2\theta} - \frac{2k_1R_0\chi}{\cos\theta}\right]^{3/2} - \left[E + \frac{k_1\chi^2}{\cos^2\theta} - \frac{2k_1R_0\chi}{\cos\theta}\right]. \quad (5)$$

The number of counts for a given pulse height, V_1, can be expressed as

$$N_{V=V_1} = \phi\sigma\, n\, A \int_0^{\chi} \int_0^{\cos^{-1}\chi/R_0} \delta(\theta_V - \theta_{V_1}) \sin\theta\, d\theta\, d\chi$$

or

$$N_{V=V_1} = \phi\,\sigma n\, A \int_0^{\chi} \sin\left[\theta(\chi, V_1)\right] d\chi \ ;$$

then we have

$$\frac{dN}{dV} = \phi\,\sigma n\ A\ \frac{d}{dV}\left[\int_0^{\chi} \sin\left[\theta\,(\chi, V)\right]\, d\chi\right],$$

where θ is defined by Eq. (5).

BIBLIOGRAPHY

1. C. Wiegand, Rev. Sci. Instr. 19, 790 (1948).
2. Hess, Patterson, and Wallace, Nucleonics 15, No. 3, 74 (1957).
3. Sugarman, Campos, and Wielgoz, Phys. Rev. 101, 388 (1946).
4. N. Bohr, Phys. Rev. 59, 270 (1941).
5. Enrico Fermi, Nuclear Physics, Notes compiled by Jay Orear, A. H. Rosenfeld, and R. A. Schluter (The University of Chicago Press, Chicago, Illinois, 1950), Chap. 2.
6. N. O. Lassen, Phys. Rev. 70, 577 (1946).
7. N. G. Utterback, C. L. Hammer, and G. H. Miller, Iowa State College, Report No. ISC-940, 1953, Ames, Iowa (Ames Laboratory AEC).
8. Brostrøm, Brøggild, and Lauritsen, Phys. Rev. 58, 651 (1940).
9. R. H. Goeckermann and I. Perlman, Phys. Rev. 76, 628 (1949).
10. B. B. Rossi and H. H. Staub, Ionization Chambers and Counters, (McGraw-Hill Book Company, Inc., New York, 1949) Chap. 1.